

# A nalytical perturbative approach to periodic orbits in the homogenous quartic oscillator potential

M B rack<sup>1</sup>, S N Fedotkin<sup>1,2</sup>, A G M agner<sup>1,2</sup> and M M ehta<sup>1,3</sup>

<sup>1</sup>Institute for Theoretical Physics, University of Regensburg, D-93040 Regensburg, Germany

<sup>2</sup>Institute for Nuclear Research, 252028 Prospekt Nauki 47, Kiev-28, Ukraine

<sup>3</sup>H arish-Chandra Research Institute, Chhatnag Road, Jhusi, Allahabad, 211019 India

May 21, 2019

## Abstract

We present an analytical calculation of periodic orbits in the homogeneous quartic oscillator potential. Exploiting the properties of the periodic Lame functions that describe the orbits bifurcated from the fundamental linear orbit in the vicinity of the bifurcation points, we use standard perturbation theory to obtain their evolution away from the bifurcation points. As an application, we derive an analytical trace formula for the density of states in a separable case, including a uniform approximation for a pitchfork bifurcation of isolated orbits occurring there, leading to full semiclassical quantization.

## 1 Introduction

The homogeneous quartic oscillator potential  $V(x; y) = ax^4 + by^4 + (-2)x^2y^2$  has been the object of several classical, semiclassical and quantum mechanical studies [1, 2, 3]. Lakshminarayan et al [4] have investigated the fixed points in Poincare surfaces of section corresponding to orbits of period four and determined empirically some of their scaling properties. Due to the homogeneity of the potential in the coordinates, orbits at different energies are related to each other through a simple scaling of coordinates and momenta. We may therefore fix the energy  $E$  at an arbitrary value. The nonlinearity parameter that regulates the dynamics is the parameter  $\epsilon$ . The system possesses periodic straight-line orbits of period one along both axes which undergo stability oscillations under variation of  $\epsilon$ . An infinite sequence of new period-one orbits bifurcates from each of these straight-line orbits, leading to almost completely chaotic dynamics [5] in the limit  $\epsilon \rightarrow 1$ .

In this letter, we specialize to the symmetric case  $a = b = 1/4$  in which the potential has  $C_{2v}$  symmetry; this potential shall in the following be denoted as the Q4 potential:

$$V_{Q4}(x; y) = \frac{1}{4}x^4 + y^4 + \frac{-2}{2}x^2y^2 : \quad (1)$$

The straight-line orbits along the  $x$  and  $y$  axes then obey identical equations of motion; we denote them as the A orbits. The dynamics of the Q4 potential (1) is invariant under the symmetry operation (cf [3])  $\epsilon \mapsto (1 + \epsilon)^2$ , which corresponds to a rotation in the  $(x; y)$  plane about 45 degrees and a simultaneous stretching of coordinates and time by a factor  $2 = (1 + \epsilon)^{1/4}$ . The limit  $\epsilon \rightarrow 1$  therefore is equivalent to the limit  $\epsilon \rightarrow 1$ . There are three values of  $\epsilon$  for which the potential is integrable: 1)  $\epsilon = 0$ , giving separability in  $x$  and  $y$ ; 2)  $\epsilon = 1$ , which is the fixed point of the above symmetry operation, giving the isotropic quartic oscillator  $V(r) = \frac{1}{4}r^4$  with  $r^2 = x^2 + y^2$ ; and 3)  $\epsilon = 3$ , giving separability after rotation about 45 degrees.

In a recent paper [6], the period-one and period-two orbits bifurcating from the A orbits have been classified completely in terms of periodic Lame functions. The motion of the A orbit along the

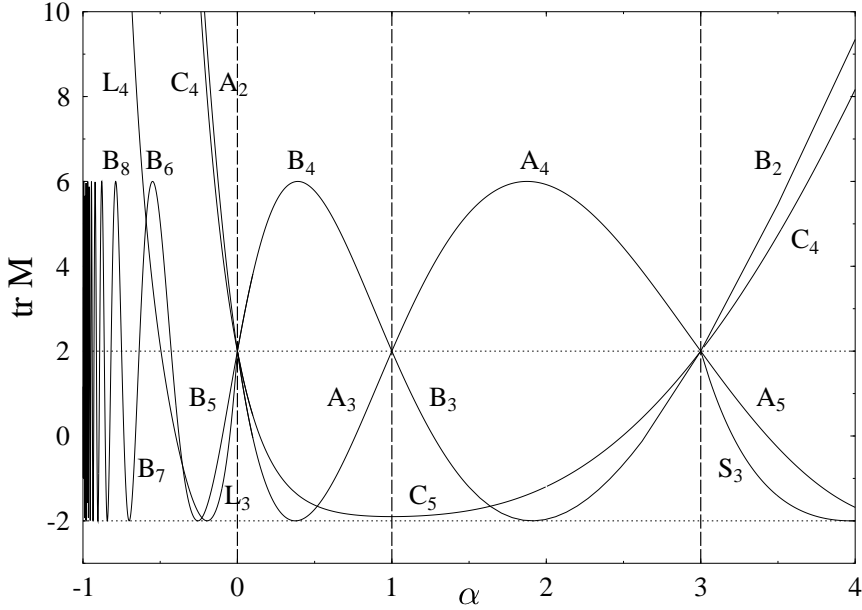


Figure 1: Stability determinant  $\text{tr}M$  of period-one orbits in the  $Q_4$  potential, plotted versus  $\alpha$ . Shown are the curves for the primitive orbits  $A$ ,  $B$  and  $C$ , and the orbits  $L$  and  $S$  bifurcating from orbits  $A$  and  $B$ , respectively. Subscripts indicate the Maslov indices. The vertical dashed lines at  $\alpha = 0, 1$  and  $3$  correspond to the integrable situations.

$y$  axis is given analytically by

$$x_A(t) = 0; \quad y_A(t) = y_0 \operatorname{cn}(y_0 t; \alpha); \quad y_0 = (4E)^{1/4}; \quad \alpha^2 = 1/2; \quad (2)$$

with the period  $T_A = 4K = y_0$ , where  $K = K(\alpha) = F(\alpha/2)$ ;  $F$  is the complete elliptic integral of the first kind with modulus  $\alpha$ , and  $\operatorname{cn}(z; \alpha)$  is one of the Jacobi elliptic functions [7]. The turning points are  $y_0$ . Note that this solution does not depend on the value of  $\alpha$ . The stability of the orbit  $A$ , however, does depend on  $\alpha$ . The linearized equation of motion in the transverse  $x$  direction yields, after transformation to the scaled time variable  $z = y_0 t$ , the Hill equation

$$x''(z) + [1 - \operatorname{sn}^2(z; \alpha)]x(z) = 0; \quad (3)$$

This is a special case of the Lamé equation [8]

$$x''(z) + \frac{h}{h - n(n+1)} \operatorname{sn}^2(z; \alpha) x(z) = 0 \quad \text{with} \quad \alpha^2 = \frac{1}{2}; \quad h = -n = \frac{1}{2}n(n+1); \quad (4)$$

We therefore know here analytically the eigenvalues  $h = -n$  of the Lamé equation, which correspond to the bifurcation points  $-n$  of the  $A$  orbit (2). This agrees with the analytical result for its stability discriminant, given by the trace of the stability matrix  $M$ , which has been derived long ago by Yoshida [9]:

$$\text{tr}M_A = 4 \cos \frac{p}{2} \sqrt{1+8} + 2; \quad (5)$$

It is easily seen that the bifurcation condition  $\text{tr}M_A = +2$  leads exactly to the values  $-n$  in (4).

In figure 1 we show the stability discriminant  $\text{tr}M$  for some period-one orbits of the  $Q_4$  potential in the interval  $1 \leq \alpha \leq 4$ . The integrable situations are indicated by the vertical dashed lines. The upper horizontal dotted line is the bifurcation line  $\text{tr}M = +2$ . The orbits  $B$  are the two straight-line orbits along the diagonals  $y = \pm x$ , which are mapped onto the  $A$  orbits under the above-mentioned symmetry operation. Their motion is given by

$$x_B(t) = y_B(t) = y_0 [2(1 + \alpha)]^{1/4} \operatorname{cn}(y_0 t; \alpha); \quad y_0 = y_0 [(1 + \alpha)/2]^{1/4}; \quad (6)$$

their period is  $T_B = T_A [2=(1 + \dots)]^{1/4}$ , and their stability discriminant  $\text{tr}M_B$  is found from  $\text{tr}M_A$  in (5) by replacing  $\lambda = (3 - \dots) = (1 + \dots)$ . The orbit C is a rotational orbit which has a discrete degeneracy of two because of time reversal symmetry; its solutions  $x_C(t)$  and  $y_C(t)$  could not be found analytically for arbitrary values of  $\lambda$  (see section 3 for the case  $\lambda = 0$ ). L and S are the first librating orbits born from A and B, respectively, in isochronous (period-one) pitchfork bifurcations. Not shown are the period-one orbits bifurcating from B for  $\lambda = 7$ . The results for  $\text{tr}M$  for the C, L and S orbits were obtained numerically. The subscripts of all the orbits shown in figure 1 denote their Maslov indices used in the semiclassical theory discussed in section 3.

The periodic solutions of the Lamé equation (4) are the Lamé functions [8, 10]  $E c_n^m(z; \lambda)$  and  $E s_n^m(z; \lambda)$  which are even and odd functions of  $z$ , respectively, with  $m$  zeros in  $z \in [0; 2K]$ . For integer  $n$  they are polynomials of degree  $n$  in the Jacobi elliptic functions  $sn$ ,  $cn$  and  $dn$ . Those with even  $m$  have the period  $T = 2K$ , those with odd  $m$  have  $T = 4K$ . For the special case  $\lambda^2 = 1/2$ ,  $m$  is fixed by  $m = [(n + 1)/2]$  and there exists only one type of Lamé polynomial,  $E c$  or  $E s$ , for each value of  $n$ . It is therefore sufficient here to denote these special polynomials by  $E_n(z)$  with  $n = 0; 1; 2; \dots$ . Their explicit expressions up to  $n = 15$  have been given in [6]. As there, we use from now on the short notation  $cn(z) = cn(z; \lambda)$ ,  $sn(z) = sn(z; \lambda)$  etc, keeping in mind that  $\lambda^2 = 1/2$ .

Nontrivial period doublings of the orbits A occur when  $\text{tr}M_A = -2$  (cf the lower horizontal line in figure 1), which leads with (5) to the critical values  $\lambda_p = 2p(p + 1) + 3/8$  with  $p = 0; 1; 2; \dots$ . The corresponding solutions of (4) with  $n = (4p + 1)/2$  are algebraic Lamé functions [11, 12] of period  $8K$  with  $m = (2p + 1)/2$ . They are discussed in [6] in connection with the period-two orbits born at the corresponding (island-chain type) bifurcations.

## 2 Perturbation expansion around bifurcation points

In the present letter, we exploit the analytical properties of the Lamé functions in order to describe the evolution of the bifurcated orbits away from the bifurcation points  $\lambda_n$ . As shown in [6], the transverse motion of the orbits bifurcated from A is, in practice, close to the bifurcation values  $\lambda_n$ , exactly described by the Lamé functions. In [6, 13] similar bifurcation cascades were investigated for Hénon-Heiles type potentials. For these it is possible to determine the amplitude of the transverse motion of the bifurcated orbits using the conservation of the total energy and the asymptotic separability of these systems near the saddle energy into motions parallel and transverse to the bifurcating orbits. However, due to the scaling property of (1) a variation of the energy does not affect the stability, and hence energy conservation cannot be exploited here in the same way. To find the evolution of the new orbits away from their bifurcations, we propose a perturbative series expansion of the equations of motion around the bifurcation points  $\lambda_n$ , leading to successive analytical expressions for the corrections to the simple (lowest-order) Lamé solutions.

The exact equations of motion for the Hamiltonian

$$H(p_x; p_y; x; y) = \frac{1}{2} (p_x^2 + p_y^2) + V_{Q4}(x; y) \quad (7)$$

with the  $Q4$  potential (1) are, in the Newtonian form,

$$x + x(x^2 + y^2) = 0; \quad y + y(y^2 + x^2) = 0; \quad (8)$$

In the following we expand the solutions of these equations around an arbitrary bifurcation point  $\lambda_n$  into Taylor series

$$x(t) = x_A(t) + x_1(t) + x_2(t) + \dots; \quad y(t) = y_A(t) + y_1(t) + y_2(t) + \dots, \quad (9)$$

whereby the small dimensionless expansion parameter  $\epsilon$  is chosen, with support from numerical evidence, as

$$\epsilon = \frac{q}{j} \quad n \in \mathbb{N}; \quad (10)$$

n	n	$E_n(z)$	$F_n(z)$
0	0	$E_0(z) = E C_0^0(z) = 1$	$F_0(z) = z$
1	1	$E_1(z) = E C_1^1(z) = \text{cn}(z)$	$F_1(z) = 2 \text{sn}(z) \text{dn}(z) \text{cn}(z) E(z)$
2	3	$E_2(z) = E S_2^1(z) = \text{dn}(z) \text{sn}(z)$	$F_2(z) = z \text{dn}(z) \text{sn}(z) \text{cn}(z)$
3	6	$E_3(z) = E S_3^2(z) = \text{cn}(z) \text{dn}(z) \text{sn}(z)$	$F_3(z) = 2 - 3 \text{cn}^4(z) - 3 \text{cn}(z) \text{sn}(z) \text{dn}(z) E(z)$

Table 1: The first four pairs of orthogonal solutions  $E_n(z)$ ,  $F_n(z)$  of the Lamé equation (4). We use the short notation  $\text{cn}(z) = \text{cn}(z; \gamma)$ ,  $\text{sn}(z) = \text{sn}(z; \gamma)$  etc; here  $\gamma^2 = 1=2$ .

As zero-order solution, we have taken  $x_A(t) = 0$  and  $y_A(t) = y_0 E_1(z)$  as given in (2) for the A orbit, since all bifurcated orbits are degenerate with the A orbit at the bifurcation points. Whereas this unperturbed solution is the same for all bifurcations, the corrections  $x_k(t)$ ,  $y_k(t)$  with  $k = 1; 2; \dots$  will depend explicitly on the value  $n$  of the chosen bifurcation point.

We now rewrite the exact equations of motion (8), singling out the value of  $n$  and replacing the difference  $n$  by  $\gamma^2$ :

$$x + n x y^2 + \gamma^2 x y^2 + x^3 = 0; \quad y + y^3 + n y x^2 + \gamma^2 y x^2 = 0; \quad (11)$$

Hereby we have chosen  $n$  which holds for all bifurcated orbits with  $n = 1$ . The orbit  $L_3$  ( $n = 0$ ) and the orbits  $F_6, P_7$  ( $n = 1=2$ , see [6]) bifurcate towards smaller values of  $\gamma$ , i.e.  $y_0 = 0$  and  $\gamma_{1=2} = 3=8$ , respectively; for these cases the sign in front of  $\gamma^2$  in the equations (11) must be reversed.

We now insert (9) into (11) and extract the equations obtained separately at each order in  $\gamma$ . This leads to a recursive sequence of linear second-order differential equations in the scaled time variable  $z$

$$x_k^{(0)}(z) + n \text{cn}^2(z) x_k(z) = h_k(z); \quad y_k^{(0)}(z) + 3 \text{cn}^2(z) y_k(z) = g_k(z); \quad k = 1; 2; 3; \dots \quad (12)$$

where the inhomogeneities on the rhs contain nonlinear combinations of  $x_{k^0}(t)$  and  $y_{k^0}(t)$  with  $k^0 < k$ . The homogeneous parts of these equations are identical to (3), (4) and have the periodic Lamé polynomials  $E_n(z)$  as solutions. According to their general theory [8, 10] the second, linearly independent solutions are non-periodic for integer  $n$ ; we shall in the following denote them by  $F_n(z)$ . We normalize them such that their Wronskians with the  $E_n$  become unity:  $\text{W}[E_n(z); F_n(z)]g = 1$ . The solutions  $E_n$  and  $F_n$  are then related to each other by [14]

$$F_n(z) = E_n(z) \int_0^z \frac{dz^0}{[E_n(z^0)]^2}; \quad E_n(z) = F_n(z) \int_z^0 \frac{dz^0}{[F_n(z^0)]^2}; \quad (13)$$

We give the lowest solutions  $E_n(z)$  and  $F_n(z)$  for integer  $n$  in table 1, where we have introduced

$$E(z) = 2E(z) \quad z = \int_0^z \text{cn}^2(u) du; \quad (14)$$

$E(z)$  is the incomplete elliptic integral of second kind, related to that of the first kind  $F(\gamma; \gamma)$  by

$$E(z) = E(\gamma; \gamma) = \int_0^z [1 - \gamma^2 \sin^2 \theta]^{1/2} d\theta; \quad z = F(\gamma; \gamma) = \int_0^z [1 - \gamma^2 \sin^2 \theta]^{1/2} d\theta; \quad (15)$$

The function  $E(z)$  in (14) is nonperiodic; its periodic part is given, with  $E = E(\gamma) = E(\frac{\pi}{2}; \gamma)$ , by

$$\text{perf}E(z)g = 2E(z) - z - \frac{2E}{2K^2} z = 2E(z) - \frac{2E}{K} z; \quad (16)$$

The last equality above follows from a known relation [7] between the complete elliptic integrals  $K$  and  $E$  for  $k^2 = 1=2$ .

For half-integer  $n$  ( appearing at the period-doubling bifurcations of the  $A$  orbits leading to the algebraic Lamé functions [11, 12] ( the linearly independent solutions  $F_n(z)$  are also periodic; the development given below must then be modified at some points. For simplicity, we limit ourselves in the following to the integer- $n$  cases occurring at the isochronous bifurcations of the  $A$  orbits.

The general solutions of the equations (12) are of the standard form

$$x_k(z) = c_k E_n(z) + d_k F_n(z) + H_k(z); \quad y_k(z) = a_k E_2(z) + b_k F_2(z) + G_k(z); \quad (17)$$

where the particular solutions of the inhomogeneous equations are given by

$$\begin{aligned} H_k(z) &= \int_0^z h_k(z^0) [F_n(z) E_n(z^0) - F_n(z^0) E_n(z)] dz^0 \\ &= E_n(z) \int_0^z du \frac{1}{[E_n(u)]^2} \int_0^u h_k(w) E_n(w) dw \end{aligned} \quad (18)$$

and

$$\begin{aligned} G_k(z) &= \int_0^z g_k(z^0) [F_2(z) E_2(z^0) - F_2(z^0) E_2(z)] dz^0 \\ &= E_2(z) \int_0^z du \frac{1}{[E_2(u)]^2} \int_0^u g_k(w) E_2(w) dw : \end{aligned} \quad (19)$$

The second parts of the above equations are useful for analytical computations. The coefficients  $a_k$ ,  $b_k$ ,  $c_k$  and  $d_k$  in (17) are determined recursively by requiring  $x_k(z)$  and  $y_k(z)$  to be periodic and to have the same symmetries as the lowest-order solutions  $y_0(z) = y_A(z)$  and  $x_1(z) = c_1 E_n(z)$ , since these symmetries cannot be changed by varying away from the bifurcations. The latter requirement leads immediately to  $a_k = 0$  for all  $k$ . Requiring  $x_k(z)$  to be periodic allows us for  $k = 3$  to determine the constant  $c_{k-2}$ , appearing in different powers on the rhs of (12), and (for any  $k$ ) the constant  $d_k$ . Periodicity of  $y_k(z)$  determines  $b_k$  in terms of the  $c_{k-2}$  with  $k^0 < k$ . We find that  $y(z)$  and  $x(z)$  are overall even and odd functions of  $z$ , respectively, so that  $c_k = d_{2k} = b_{2k+1} = 0$  and hence  $x_{2k}(z) = y_{2k+1}(z) = 0$  for  $k = 0; 1; 2; \dots$ : All integrals can be done analytically.

Up to this point, the solutions  $y_k(z)$  and  $x_k(z)$  all have the same period  $T_A$  as the  $A$  orbit. However, the bifurcated orbits will have different periods away from the bifurcation points  $z_n$ . We found that the easiest way to take this effect into account is an *a posteriori* rescaling of the dimensionless argument  $z = y_0 t$  in the above solutions. At a given order of the perturbation expansion, we set  $z = w t$  and determine the value of  $w$  by the expansion of the new periods

$$T = \frac{4K}{w} = T_A + T_1 + T_2 + \dots \quad (20)$$

leading to

$$w = y_0 \left( 1 + (T_1 - T_A) + (T_2 - T_A) + \dots \right)^{-1} \quad (21)$$

The coefficients  $T_k$  in this expansion can be determined by writing the total energy in terms of the series (9) as

$$E = \frac{1}{2} (x^2 + y^2) + \frac{1}{4} (x^4 + y^4) + \frac{1}{2} x^2 y^2 = E_0 + E_1 + E_2 + \dots; \quad (22)$$

inserting the above solutions for  $x_k(wt)$  and  $y_k(wt)$  with  $w$  given by (21), and using the fact that we keep the energy  $E$  constant while varying  $w$ . We find for all investigated orbits that  $T_1 = T_2 = T_3 = 0$  and  $T_4 \neq 0$ , so that  $T$  varies with  $w$  like

$$T(w) = T_A + (w - w_0)^2 T_4 + \dots \quad (23)$$

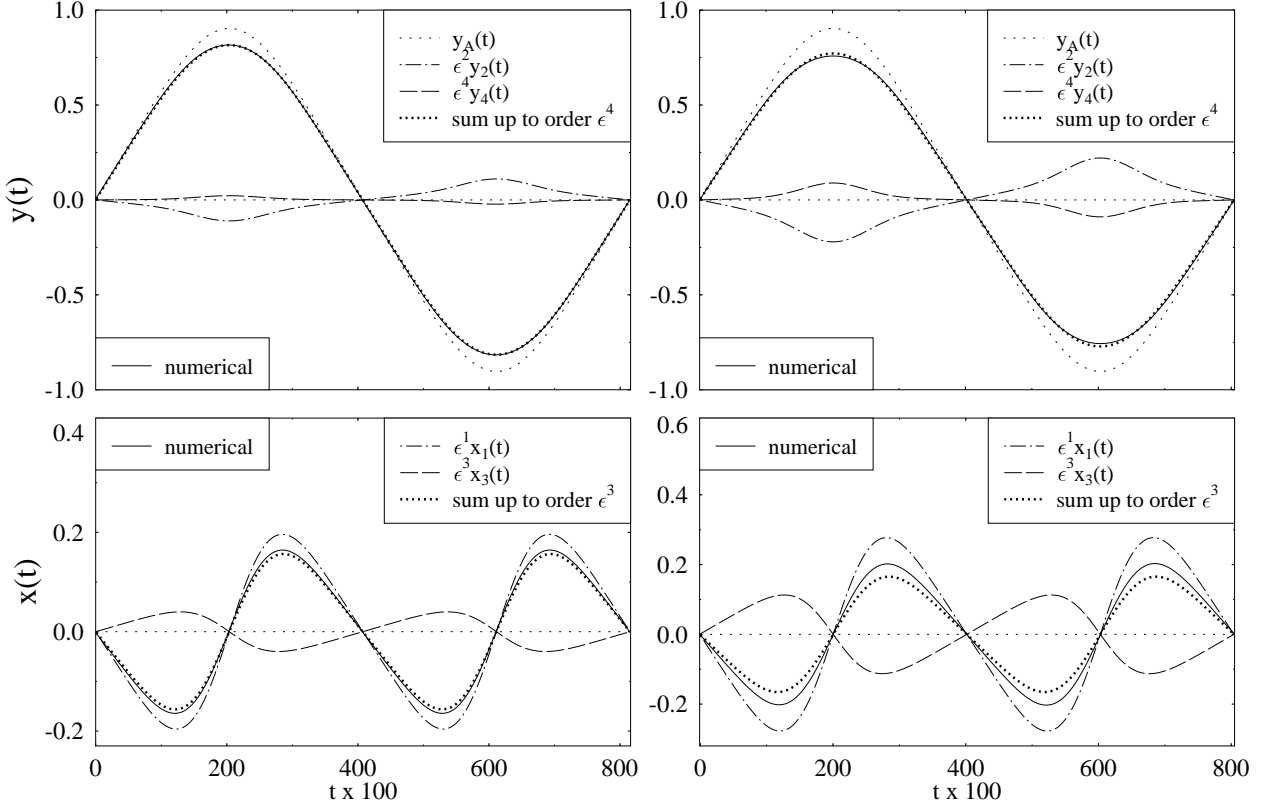


Figure 2: Coordinates  $x(t)$  and  $y(t)$  of the orbit  $R_5$ , evaluated at  $p = 7$ ,  $i\epsilon = 1$  (left side) and  $p = 8$ ,  $i\epsilon = \frac{1}{2}$  (right side). Solid lines: numerical results. Heavy dotted lines: perturbation series (9) summed up to 3rd and 4th order for  $x(t)$  and  $y(t)$ , respectively. Other lines give partial contributions as labeled by the inserts. (Units such that  $h = 1$ ;  $E = 1=6$ .)

As an illustration of our method, we present the results for the orbit  $R_5$  born at  $p = 6$  and existing only for  $p = 6$ . We obtain the following analytical solutions up to order  $\epsilon^4$  (with  $z = wt$ )

$$\begin{aligned}
 x_1(t) &= c_1 \operatorname{sn}(z) \operatorname{dn}(z) \operatorname{cn}(z); & x_3(t) &= c_1 \operatorname{sn}(z) \operatorname{dn}(z) \operatorname{cn}(z) \frac{25}{132} + \frac{7}{180} \operatorname{cn}^4(z); \\
 y_0(t) &= y_0 \operatorname{cn}(z) = y_A(z); & y_2(t) &= \frac{c_1^2}{4y_0} \operatorname{cn}(z) [1 + \operatorname{cn}^4(z)]; \\
 y_4(t) &= \frac{c_1^2}{y_0} \operatorname{cn}(z) \frac{1}{10080} \operatorname{cn}^7(z) - 206 \operatorname{cn}^4(z) + 111 \operatorname{cn}^8(z) + \frac{5}{264} \frac{h}{1 + \operatorname{cn}^4(z)} \operatorname{cn}^5(z);
 \end{aligned}$$

where  $c_1 = y_0 \frac{p}{11=45}$  and the lowest nonzero correction to the period is  $T_4 = (11=1260) T_A$  so that  $w = y_0 [1 - (11=1260)^4]$ . In figure 2 we compare the results obtained by summing the above analytical results according to (9) up to order  $\epsilon^4$ , shown by the heavy dotted lines, with the results obtained by numerical solution of the exact equations of motion (8), shown by the solid lines. The single contributions obtained at each order in  $\epsilon$  are shown by the other lines, as labeled by the inserts. The left panels are calculated for  $p = 7$  where  $i\epsilon = 1$ , and the right panels for  $p = 8$  where  $i\epsilon = \frac{1}{2}$ . The convergence is surprisingly good even when the expansion parameter  $\epsilon$  is larger than unity. This is due to the rapidly decreasing amplitudes of the  $x_k(z)$  and  $y_k(z)$  with increasing  $k$ . Note that for  $y(t)$ , where the agreement is perfect for  $i\epsilon = 1$  and still very good for  $i\epsilon = \frac{1}{2}$ , we have included three terms, whereas  $x(t)$  only contains two terms. Obtaining  $x_5(z)$  would have required to calculate both  $y_6(z)$  and  $x_7(z)$  and to make them periodic, which [though analytically possible] would have been rather cumbersome.] However, the fact that the remaining errors in  $x(t)$  are of the same order as  $\operatorname{cn}^4(z)$  suggests that adding the third term  $x_5(z)$  would lead to an equally good convergence for  $x(t)$ . Similar results were also obtained for other bifurcated orbits.

### 3 Semiclassical trace formula for $\epsilon = 0$

In this section we shall apply our method to derive an analytical semiclassical trace formula for the density of states of the separable  $Q_4$  potential at  $\epsilon = 0$ . Although this is an integrable system and WKB (or torus) quantization can be applied straightforwardly, it contains a subtle detail in that there exists here a bifurcation of an isolated orbit. As we see from figure 1 the orbit  $A$ , which is stable ( $A_3$ ) for  $0 < \epsilon < 1$ , becomes unstable ( $A_2$ ) for  $\epsilon < 0$ ; the orbit  $L_3$  bifurcating from it exists only for  $\epsilon > 0$  and is stable for  $0.5 < \epsilon < 0$ . We will show below that the existence of these isolated orbits affects the quantum spectrum at  $\epsilon = 0$ . We demonstrate this by calculating the semiclassical trace formula for the density of states with different degrees of coarse-graining and comparing it to the corresponding quantum mechanical results. The exact quantum spectrum has been obtained by diagonalization of (1) in a harmonic oscillator basis.

Straightforward WKB quantization gives the approximate spectrum  $(n_x; n_y = 0; 1; 2; \dots)$

$$E_{n_x n_y}^{\text{WKB}} = (1=4) (6 h=4K)^{4=3} \sum_{i=1}^{\infty} (n_x + 1=2)^{4=3} + (n_y + 1=2)^{4=3} : \quad (24)$$

From this we obtain in the standard way [15, 16] the following Berry-Tabor type trace formula, to leading order in  $h$ , for the oscillating part of the semiclassical density of states:

$$q_{\text{sc}}^{\text{2D}}(E) = \frac{4K}{2h} \sum_{n,m=1}^{3=2} (4E)^{1=8} \sum_{k=1}^{\infty} (-1)^{n+m} \frac{nm}{(n^4 + m^4)^{5=8}} \cos \frac{1}{h} S_{nm}(E) - \frac{1}{4} : \quad (25)$$

The classical actions

$$S_{nm}(E) = (4K=3) (4E)^{3=4} (n^4 + m^4)^{1=4} \quad (26)$$

of the two-dimensional (2D) rational tori  $(n; m)$  correspond to the periodic orbits

$$x(t) = w_x \cos(w_x t + \phi); \quad y(t) = w_y \cos(w_y t); \quad (27)$$

with

$$w_x = (4E)^{1=4} n (n^4 + m^4)^{1=4}; \quad w_y = (4E)^{1=4} m (n^4 + m^4)^{1=4}; \quad (28)$$

These orbits form degenerate families described by the parameter  $2 \pi [0; 4K]$ . The  $(n; n)$  resonances are the families containing the  $n$ th repetitions of the orbits  $B$  (for  $\epsilon = 0$  or  $2K$ ) and  $C$  (for  $\epsilon = K$  or  $3K$ ). Summation over all resonances  $(n; m)$  with  $n, m > 0$  yields the trace formula (25).

However, the system also contains the isolated resonances  $(n; 0)$  and  $(0; m)$  with  $n, m = 1, 2, 3, \dots$  which correspond to the (repeated) one-dimensional  $A$  orbit in the  $x$  and  $y$  direction. The Gutzwiller trace formula [17] for isolated orbits cannot be used to describe this orbit because of its bifurcation at  $\epsilon = 0$ . However, the uniform approximation for a generic pitchfork bifurcation [18, 19] can here be applied to describe the bifurcating system of orbits  $A_3 \rightarrow A_2 + L_3$  and all their repetitions. Their Maslov indices agree with the rules given in [19]. The factor 2 appearing in the period doubling for the generic case here plays the role of an extra degeneracy factor 2 of the bifurcated  $L_3$  orbits, which is due to the reflection symmetries of the  $Q_4$  potential at the symmetry axes containing the  $A$  orbits. This gives the following common contribution of the  $A$  and  $L$  orbits to the trace formula

$$q_{\text{sc}}^{\text{bif}}(E) = \frac{(4K)^{3=4}}{(h)^{5=4}} (4E)^{1=16} \sum_{n=1}^{\infty} (-1)^n \frac{1}{n^{3=4}} \cos \frac{n}{h} S_A(E) - \frac{3}{8} ; \quad (29)$$

where  $S_A(E) = (4K=3) (4E)^{3=4}$  is the action of the primitive  $A$  orbit. Hereby we have made use of the method of the previous section to obtain the coefficient  $T_4 = T_A (3^2 = 16K^4)$  of the  $L_3$  orbit, which determines the constant  $a$  appearing in equation (16) of [19] and leading to (29).

Comparing the results (25) and (29), we see that the latter is of order  $h^{1=4}$  relative to the leading-order contributions of the 2D torus families. For isolated orbits, this relative factor would be  $h^{1=2}$ ; the difference here is due to the bifurcation. It is therefore not surprising that the bifurcating orbits have a non-negligible influence on the density of states (at least for low energies, where the negative power of  $E$  in the amplitude of (29) does not suppress their contribution too much).

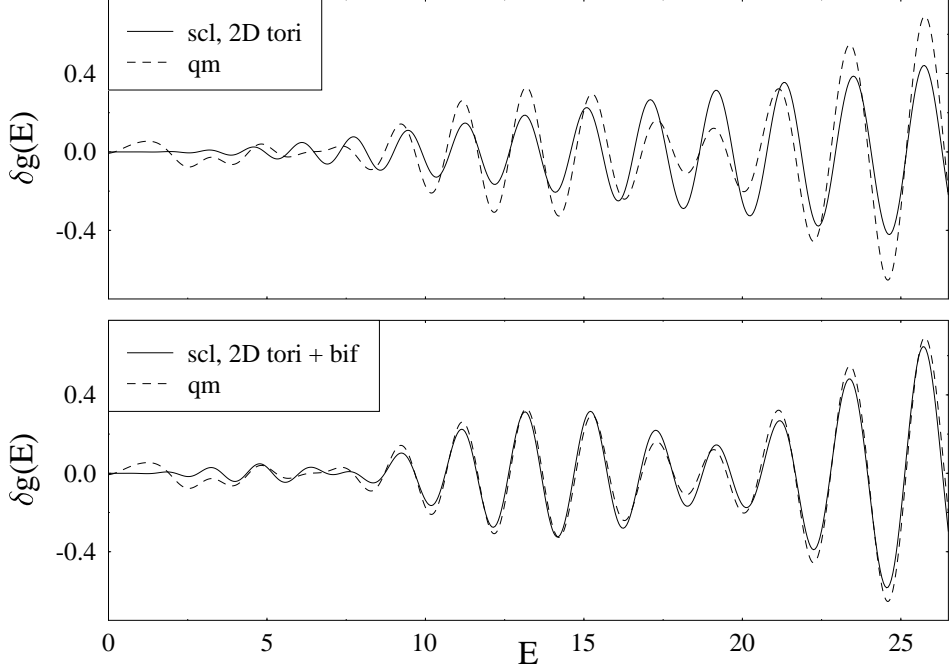


Figure 3: Oscillating part of the coarse-grained density of states of the Q 4 potential at  $\epsilon = 0$  (units such that  $h = 1$ ; Gaussian smoothing width  $\sigma = 1$ ). Dashed lines: quantum-mechanical results (30). Solid lines: semiclassical results with  $n_{\max} = m_{\max} = 2$ . Upper panel: using only the contribution (25) of the 2D tori; lower panel: including also the contribution (29) from the bifurcating orbits.

In our numerical calculations, we coarse-grain both the semiclassical and the exact density of states by convoluting them with a normalized Gaussian  $\exp(-\frac{(E - E_{\text{center}})^2}{2\sigma^2})$ . For larger values of  $\sigma$ , this suppresses the longer periodic orbits but still preserves the prominent gross-shell structure in the density of states; in the limit  $\sigma \rightarrow 0$ , the sum of delta functions is recovered. The quantum-mechanical expression for the coarse-grained  $\delta g(E)$  is then given in terms of the exact quantum spectrum  $E_{n_x n_y}$  by

$$g_{\text{qm}}(E) = \frac{1}{p} \sum_{n_x n_y} \exp(-\frac{(E - E_{n_x n_y})^2}{2\sigma^2}) = \frac{p}{2} g_{\text{TF}}(E); \quad (30)$$

where  $g_{\text{TF}}(E)$  is the average density of states which for the Q 4 potential can be obtained analytically in the Thomas-Fermi approximation for any  $\epsilon > 1$ :

$$g_{\text{TF}}(E) = (2\pi h^2) K(q) \frac{p}{E}; \quad q = \frac{\sqrt{1 - \epsilon}}{(1 - \epsilon)^{1/2}}; \quad (\epsilon > 1) \quad (31)$$

and, for  $\epsilon = 0$ , becomes

$$g_{\text{TF}}(E) = (2K = h^2) \frac{p}{E}; \quad (\epsilon = 0) \quad (32)$$

In the semiclassical trace formulae, the coarse-graining leads to an extra factor  $\exp(-\frac{(T_{\text{po}} - 2h)^2}{2\sigma^2})$  under the periodic orbit sum, whereby  $T_{\text{po}} = dS_{\text{po}}(E)/dE$  are the periods of the orbits.

In Figure 3 we show the coarse-grained level densities obtained with  $\sigma = 1$  (in units such that  $h = 1$ ); the periodic orbit sums in (25) and (29) can here be limited by  $n_{\max} = m_{\max} = 2$ . In the upper panel, the semiclassical result contains only the contribution (25) of the 2D tori. This is seen to lead to a monotonic increase of the amplitude of the oscillations, whereas the quantum result shows a clear beating structure. When including the contribution (29) of the bifurcating orbits in the semiclassical result, shown in the lower panel, the quantum result is nicely reproduced. Since mainly the orbits with  $n = m = 1$  contribute here, the quantum beat is clearly the result of the interference between the (1,1) torus family on one hand and the primitive isolated orbits A and L, taking part in the bifurcation, on the other hand.

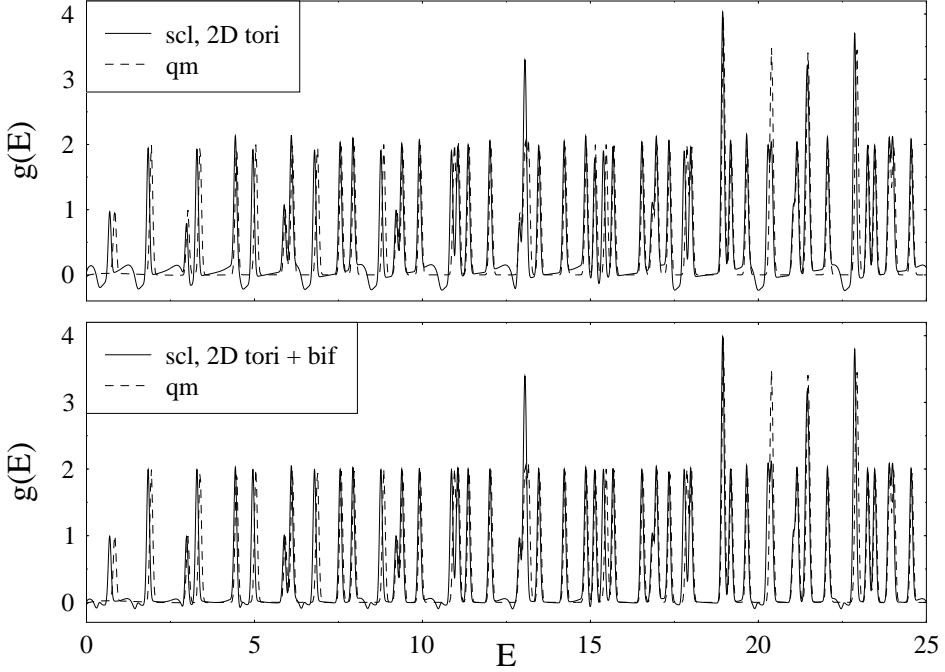


Figure 4: The same as figure 3, but for the total density of states including the average part (32), with  $\epsilon = 0.06$ . Periodic orbit sums are cut at  $n_{\text{max}} = m_{\text{max}} = 30$ .

The effect of the bifurcating orbits is less dramatic when we choose a finer resolution of the energy spectrum, obtained with a smaller value of  $\epsilon$ . In figure 4 we show the total density of state, including the average part (32), obtained for  $\epsilon = 0.06$ . Hereby periodic orbits up to  $n_{\text{max}} = m_{\text{max}} = 30$  contribute to the semiclassical results. We have normalized  $g(E)$  hereby the factor  $\epsilon^2$  so that the quantum result exhibits the correct degeneracies 1 or 2. Some apparently wrong higher degeneracies are badly resolved accidental (near-)degeneracies. At first glance there is not much of a difference between the upper and lower panels of figure 4. However, a closer inspection reveals that the semiclassical degeneracies are wrong, with errors of up to 20%, in the upper part where only the 2D tori are included, whereas they become practically exact when including the bifurcating isolated orbits in the lower panel. There also the bottom regions between the peaks are improved, the remaining small oscillations being numerical noise. Note that the inclusion of the bifurcating orbits does not affect the peak positions of the semiclassical curves, which are exactly those of the spectrum  $E_{nm}^{\text{WKB}}$  given in (24). The shifts in the peaks seen at the lowest energies are due to the typical errors inherent in the WKB approximation, which rapidly decrease with increasing energy.

## 4 Summary

We have formulated a perturbative scheme to calculate analytically the shapes of periodic orbits bifurcating from the straight-line orbits in the quartic oscillator potential, exploiting the properties of the periodic Lamé functions in terms of Jacobi elliptic functions. For period-one orbits we are able to give analytical expressions of the resulting perturbative series. Even when the perturbation parameter  $\epsilon$  is slightly larger than unity, satisfactory convergence to the numerically obtained solutions is reached by going up to order  $\epsilon^4$ , where the necessary algebraic work is not too cumbersome. For the period-two orbits born at period-doubling bifurcations, the algebraic Lamé functions have to be used; the repeated integrations arising in the perturbation expansion then became more difficult and we could not do all of them analytically. Resorting to numerical integrations, however, whereby the coefficients  $b_k$ ,  $c_k$  and  $d_k$  in (17) were determined numerically by iteration, we could reach a similar convergence.

In section 3 we have shown that the semi-classical trace formula

$$g_{sc}(E) = g_{TF}(E) + g_{sc}^{2D}(E) + g_{sc}^{bif}(E); \quad (33)$$

using the analytical expressions (25), (29) and (32) for the three contributions, gives a very good approximation to the exact quantum mechanical density of states of the quartic oscillator at  $\epsilon = 0$ . Its low-frequency part, extracted with an energy coarse-graining parameter  $\epsilon = 1$ , reveals a strong quantum beat. This beat can only be reproduced semi-classically when the shortest periodic orbit families, contributing through  $g_{sc}^{2D}(E)$ , are allowed to interfere with the isolated orbits A and L, taking part in a pitchfork bifurcation and contributing through  $g_{sc}^{bif}(E)$  in a known uniform approximation. The high-resolution spectrum is dominated by the Berry-Tabor part  $g_{sc}^{2D}(E)$  which yields exactly the peaks corresponding to the WKB spectrum. The quantum degeneracies are, however, substantially affected by the contributions from the bifurcating orbits. An alternative treatment of the bifurcating orbits will be discussed in a forthcoming publication.

We are grateful to Christian Ammann for the numerical computation of the quantum spectrum. SNF, AGM and MM acknowledge the hospitality of the University of Regensburg during their research visits. This work has been supported by the Deutsche Forschungsgemeinschaft.

## References

- [1] Eckhardt B 1988 *Phys. Rep.* 163 205  
Eckhardt B, Høøe G and Pollak E 1989 *Phys. Rev. A* 39 3776
- [2] Bohigas O, Tomsovic S and Ullmo U 1993 *Phys. Rep.* 223 43
- [3] Eriksson A B and Dahlqvist P 1993 *Phys. Rev. E* 47 1002
- [4] Lakhshminarayanan A, Santhanam M S and Sheorey V B 1996 *Phys. Rev. Lett.* 76 396
- [5] Dahlqvist P and Russberg G 1990 *Phys. Rev. Lett.* 65 2837
- [6] Brack M, Mehta M and Tanaka K 2001 *J. Phys. A* 34 8199
- [7] Gradshteyn IS and Ryzhik IM 1994 *Table of Integrals, Series, and Products* (Academic Press, New York, 5th edition) ch 8.1
- [8] Erdelyi A et al 1955 *Higher Transcendental Functions* vol 3 (New York: McGraw-Hill) ch 15
- [9] Yoshida H 1984 *Celest. Mech.* 32 73
- [10] Ince E L 1940 *Proc. R. Soc.* 60 47
- [11] Ince E L 1940 *Proc. R. Soc.* 60 83
- [12] Erdelyi A 1941 *Phil. Mag.* 32 348
- [13] Brack M 2001 *Foundations of Physics* vol 31, ed A Inomata et al p 209 (*Festschrift in honor of the 75th birthday of Martin Gutzwiller*)  
(Brack M 2000 LANL preprint [nlin/0006034](http://arxiv.org/abs/nlin/0006034))
- [14] Whittaker E T and Watson G N 1969 *A course of modern analysis* 4th edn (Cambridge: University Press)
- [15] Berry M V and Tabor M 1976 *Proc. R. Soc.* 349, 101
- [16] Creagh S C and Littlejohn R G 1992 *J. Phys. A* 25, 1643
- [17] Gutzwiller M C 1971 *J. Math. Phys.* 12 343
- [18] Oзорио де Амейда A M and Hannay J H 1987 *J. Phys. A* 20 5873
- [19] Schomerus H and Sieber M 1997 *J. Phys. A* 30 4537